Geophysical Research Letters

RESEARCH LETTER
10.1029/2019GL083888

The 27-Day Solar Rotational Cycle Response in the Mesospheric Metal Layers at Low Latitudes

J. Wu[1,2,3], W. Feng[2,4], X. Xue[1,3,5], D. R. Marsh[2,6], J. M. C. Plane[2], and X. Dou[1,7]

[1]CAS Key Laboratory of Geospace Environment, School of Earth and Space Sciences, University of Science and Technology of China, Hefei, China, [2]School of Chemistry, University of Leeds, Leeds, UK, [3]CAS Center for Excellence in Comparative Planetology, Hefei, China, [4]National Center for Atmospheric Science, University of Leeds, Leeds, UK, [5]Mengcheng National Geophysical Observatory, School of Earth and Space Sciences, University of Science and Technology of China, Hefei, China, [6]National Center for Atmospheric Research, Boulder, CO, USA, [7]Hefei National Laboratory for the Physical Sciences at the Microscale,University of Science and Technology of China, Hefei, China

Key Points:
- First study of the response of metal layers in the mesosphere and lower thermosphere to the 27-day solar rotational cycle
- Sensitivity of the Na, K, and Fe layers varies with altitude for different metals (up to −5% change for 10% change in SSI at Lyman-alpha)
- Tentative evidence for the 27-day cycle in 10-year satellite observations of the Na layer

Supporting Information:
- Supporting Information S1
- Figure S1
- Figure S2
- Figure S3
- Figure S4

Correspondence to:
J. Wu and X. Xue,
wujf@ustc.edu.cn; xuexh@ustc.edu.cn

Citation:
Wu, J., Feng, W., Xue, X., Marsh, D. R., Plane, J. M. C., & Dou, X. (2019). The 27-day solar rotational cycle response in the mesospheric metal layers at low latitudes. *Geophysical Research Letters*, *46*. https://doi.org/10.1029/2019GL083888

Received 27 MAY 2019
Accepted 18 JUN 2019
Accepted article online 24 JUN 2019

Abstract To investigate the response of the meteoric metal layers in the mesosphere and lower thermosphere regions to the 27-day solar rotational cycle, a long-term simulation of the Whole Atmosphere Community Climate Model with the chemistry of three metals (Na, K, and Fe) was analyzed. The correlation between variability in the metal layers and solar 27-day forcing during different phases of the solar 11-year cycle reveals that the response in the metal layers is much stronger during solar maximum. The altitude-dependent correlation and sensitivity of the metal layers to the solar spectral irradiance demonstrates that there is a significant increase in sensitivity to solar rotational cycle with increasing altitude. Above 100 km, the sensitivity of the metals to changes of 10% in the solar spectral irradiance at Lyman-alpha is estimated to be −5%. A similar response is seen in Na layer measurements made by the Optical Spectrograph and InfraRed Imaging System instrument on the Odin satellite.

1. Introduction

Compared to the lower atmosphere, the upper mesosphere and lower thermosphere (MLT) region is a challenging region of the atmosphere to study because of the relative paucity of observations. Nevertheless, the MLT is a key region of the near-Earth space environment, with electrodynamical and radiative processes from above and dynamical processes arising from a variety of upward propagating atmospheric waves from below (e.g., see Dawkins et al., 2016; Plane et al., 2015; Yigit et al., 2016).

There has been a long-term interest in the influence of the solar cycle in the upper atmosphere and possible ways in which it could couple downward to influence climate. However, due to the paucity of long-term (multidecade) observations in the MLT, it is actually quite difficult to determine how the atmosphere responds to the solar cycle. In response to this, researchers have studied how composition and dynamics vary on shorter solar timescales, in particular the solar rotation variation, that is, the 27-day cycle. However, extracting a clean 27-day response in MLT composition has proved difficult due to the small amplitude of the signal. For example, Keating et al. (1987) determined ozone increased by only 0.1% for a 1% increase in Lyman-α at 80 km. This motivates looking for the 27-day signal in other MLT parameters. Over the past few decades, a number of satellite observations and models have been used to look at the 27-day variations in composition in the MLT. For example, the response of mesopause temperatures (von Savigny et al., 2012), the hydroxyl radical and water vapor (Shapiro et al., 2012), atomic oxygen (Lednyts'kyy et al., 2017), standard phase heights (von Savigny et al., 2019), and noctilucent clouds (Robert et al., 2010; Thurairajah et al., 2017) to the solar 27-day cycle have been studied.

One area that has not been explored before is the 27-day response of the meteoric metal layers (e.g., Na, K, and Fe). Metal layers are produced in the MLT by meteoric ablation and, because they can be observed by ground-based lidar and spaceborne spectroscopy, are widely used as tracers for chemical and dynamical processes that occur within this region of the atmosphere (Plane et al., 2015). The metal composition in the MLT is dependent on the interaction of photochemical reactions, chemical reactions, dynamics, and electrodynamics. Among these processes, solar radiation affects not only the photo-ionization and photolysis rates but also the chemical reactions with other chemical components (e.g., O, O_2, O_3, and OH). Therefore, understanding the influence of solar activity on the metal layers is one of the keys to understanding

solar-terrestrial coupling, and the accurate models and continuous observations of such metal layers enable us to investigate such processes (Dawkins et al., 2016, 2014; Feng et al., 2013; Marsh et al., 2013; Plane et al., 2014). Dawkins et al. (2016) studied the response of the Na, K, and Fe layers to the 11-year solar cycle by comparing observations from the Optical Spectrograph and InfraRed Imaging System (OSIRIS) on the Odin satellite, with simulations from the Whole Atmosphere Community Climate Model (WACCM) containing interactive Na, K, and Fe chemistry. In contrast, examining the response to short-term solar variations is more challenging because of the need for continuous spatiotemporal sampling with a small observational uncertainty. Thus, simulations with a whole atmosphere model are a feasible first step for investigating the response of metal layers within the MLT region to the 27-day solar cycle.

The scope of this paper is to examine the response of the Na, K, and Fe layers in the MLT to the 27-day solar cycle, using WACCM simulations. The paper is organized as follows: A brief description of the model data is given in section 2; the results of the cross-correlation analysis and superposed epoch analysis (SEA) for the metal layers are discussed in section 3, along with a parallel analysis of OSIRIS Na observations; and section 4 contains the conclusions.

2. Data Description and Analysis

In this study, output from a free-running version of WACCM is analyzed for solar-driven 27-day variations of the Na, K, and Fe metal layers. WACCM is a climate chemistry model framed by the Community Earth System Model (Hurrell et al., 2013) developed by the National Center for Atmospheric Research, and the key chemistry and dynamical features are described in detail in Marsh et al. (2013). Validated metal chemistry modules for Na (Marsh et al., 2013), K (Plane et al., 2014), and Fe (Feng et al., 2013) are added. The vertical resolution in the MLT is ~3.5 km, and model output frequency is 30 min for selected stations. The prescribed daily solar spectral irradiance (SSI;Lean et al., 2005) and energetic particle precipitation are also included (Marsh et al., 2013).

Data analysis is focused on the daytime (0800 to 1600 LT) average of the metal layers over the Arecibo site (18.3° N, 293.2° E). The low-latitude Arecibo site was chosen in order to avoid the influence of energetic particle precipitation which might interfere with the underlying 27-day cycle, and this region is also the most directly affected by the solar irradiance. The data sets of a few stations located in middle and high latitudes were also analyzed. However, the correlation with 27-day solar cycle weakened with increasing latitude, and the analysis of latitude response is beyond the scope of this article.

In this study we use the SSI at Lyman-alpha (121.5-nm wavelength) as a proxy indicator for the ultraviolet (UV) solar irradiance. The long-term simulation lasts for 50 years (1955–2005), and we then analyzed the SSI during this period using wavelet analysis (Torrence & Compo, 1998). The power spectrum reveals a highly pronounced 27-day solar cycle during the solar maximum phase of solar cycle 22 (1989–1994). To directly examine the metal layer response to the 27-day cycle during solar minimum and solar maximum periods, we calculated the data anomaly between 1984 and 1988 for solar minimum and the anomaly from 1989 to 1994 for solar maximum (see section 3). The time evolution of the wavelet power at a period of 27 days of the SSI anomaly for the years from 1984 to 1994 is presented in supporting information Figure S1.

In order to test the response to the 27-day solar cycle predicted by the model, we use the Na atomic density retrieved from the OSIRIS instrument on the Odin satellite (Gumbel et al., 2007; Fan et al., 2007). Here OSIRIS Na data are daily averaged over the tropics (27° S–27° N) from 2004 to mid-2013, spanning portions of solar cycles 23 and 24. Although the solar cycle 24 is unusually quiet (e.g., Singh & Tonk, 2014), observations can still be used to test the model result.

3. Results and Discussion

In order to remove the influence of long-term trends and very short-term fluctuations and to focus on the response to the 27-day solar cycle, we subtracted the 60-day running mean from the daily irradiance and model output and then performed a 3-day running mean smoothing to obtain the anomaly. Figure 1 presents an example of the running mean method applied to the WACCM K partial column density above 110 km and SSI. There is a clearly visible and statistically significant anticorrelation between the K and SSI index anomaly time series (Figure 1b), with a maximum negative cross-correlation coefficient of −0.53 (significant at the 99.9% confidence level) at a time lag of 0 days.

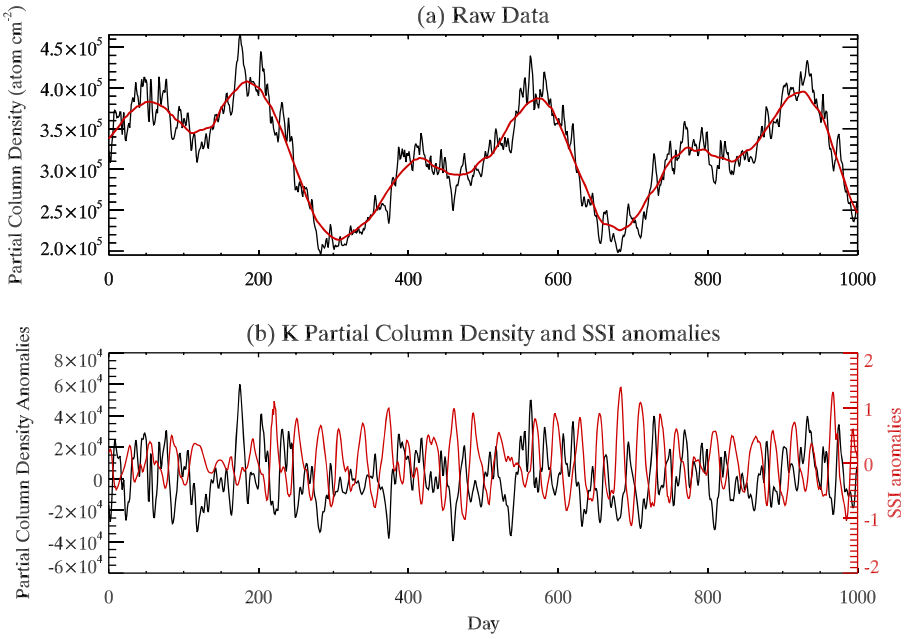

Figure 1. (a) Time series of daily averaged Whole Atmosphere Community Climate Model-K partial column density above 110 km above Arecibo from 1989 (black line) and 60-day running mean (red line) for the time period analyzed. (b) K and SSI index anomalies obtained by subtracting a 60-day running mean from the time series (smoothed with a 3-day running mean filter). SSI = solar spectral irradiance.

The cross correlation as a function of lag of the anomaly of the modeled Na, K, and Fe atoms in mixing ratio and temperature at Arecibo versus SSI anomaly are presented in Figure 2, for solar maximum (left panel) and solar minimum (right panel). Na, K, and Fe atoms all show a strong anticorrelation (correlation coefficients up to −0.5) with essentially no time lag at heights above ~100 km, while the corresponding temperature shows a positive correlation in the same altitude range (Figure 2g). As discussed in Plane et al. (2015), ion chemistry dominates above 100 km, and the rate of direct photo-ionization, as well as charge transfer with ambient NO^+ and O_2^+ ions, increases with increasing UV solar irradiance. Metal atoms are therefore converted more rapidly to metal ions. Of course, the increased electron concentration, which essentially balances the NO^+ and O_2^+ concentrations to preserve charge neutrality (metallic ions are a minor component, apart from in sporadic E layers), should also lead to faster dissociative recombination of molecular metal-containing ions (e.g., $Na^+{\cdot}N_2$ and FeO^+) to produce metal atoms. Thus, the rates of ionization and neutralization would both speed up by essentially the same factor, so the balance between neutral metal atoms and metal ions would be approximately constant. However, other factors play a role.

First, increased extreme ultraviolet (EUV) radiation causes an increase in the atomic O mixing ratio (i.e., a positive correlation with SSI above 120 km; Figure S2b). O reduces molecular ions back to atomic metal ions (e.g., $FeO^+ + O \rightarrow Fe^+ + O_2$), and thus prevents dissociative recombination to neutral metal atoms (Plane et al., 2015). Interestingly, the cross correlation between the WACCM daytime O density anomaly and SSI shows a time lag of 13 days (Figure S2a), which is in good agreement with the observations of Lednyts'kyy et al. (2017). Second, the O_3 mixing ratio (and density) are anticorrelated with SSI (Figures S2c and S2d). In the case of Fe^+, the reaction with O_3 to form FeO^+, which is the first step above 100 km for converting Fe^+ to Fe, will therefore be slower, reinforcing the anticorrelation of Fe with SSI. Lastly, the strong correlation of temperature with SSI (Figure 2g) means that at zero time lag, the recombination reactions which form clusters (e.g., $Na^+ + N_2\ (+ N_2) \rightarrow Na^+{\cdot}N_2$) which then dissociatively recombine with electrons, and dielectronic recombination of the metal ions with electrons (e.g., $Na^+ + e^- \rightarrow Na + h\nu$) get slower because their rate coefficients have negative temperature dependences (Plane et al., 2015).

All these factors explain why the metal layers above 100 km are anticorrelated with solar irradiance. At the metal peak height (~91 km for Na and K and ~87 km for Fe, see, e.g., Plane et al., 2015), neutral chemistry dominates. The simulated temperature exhibits a weak (though still significant) positive correlation with the 27-day solar cycle around 90 km (Figure 2g). For Na and Fe, the rate coefficients for the reactions which release the metal atoms from their reservoirs ($NaHCO_3 + H \rightarrow Na + H_2CO_3$; $FeOH + H \rightarrow Fe + H_2O$) increase with rising temperature (i.e., have positive activation

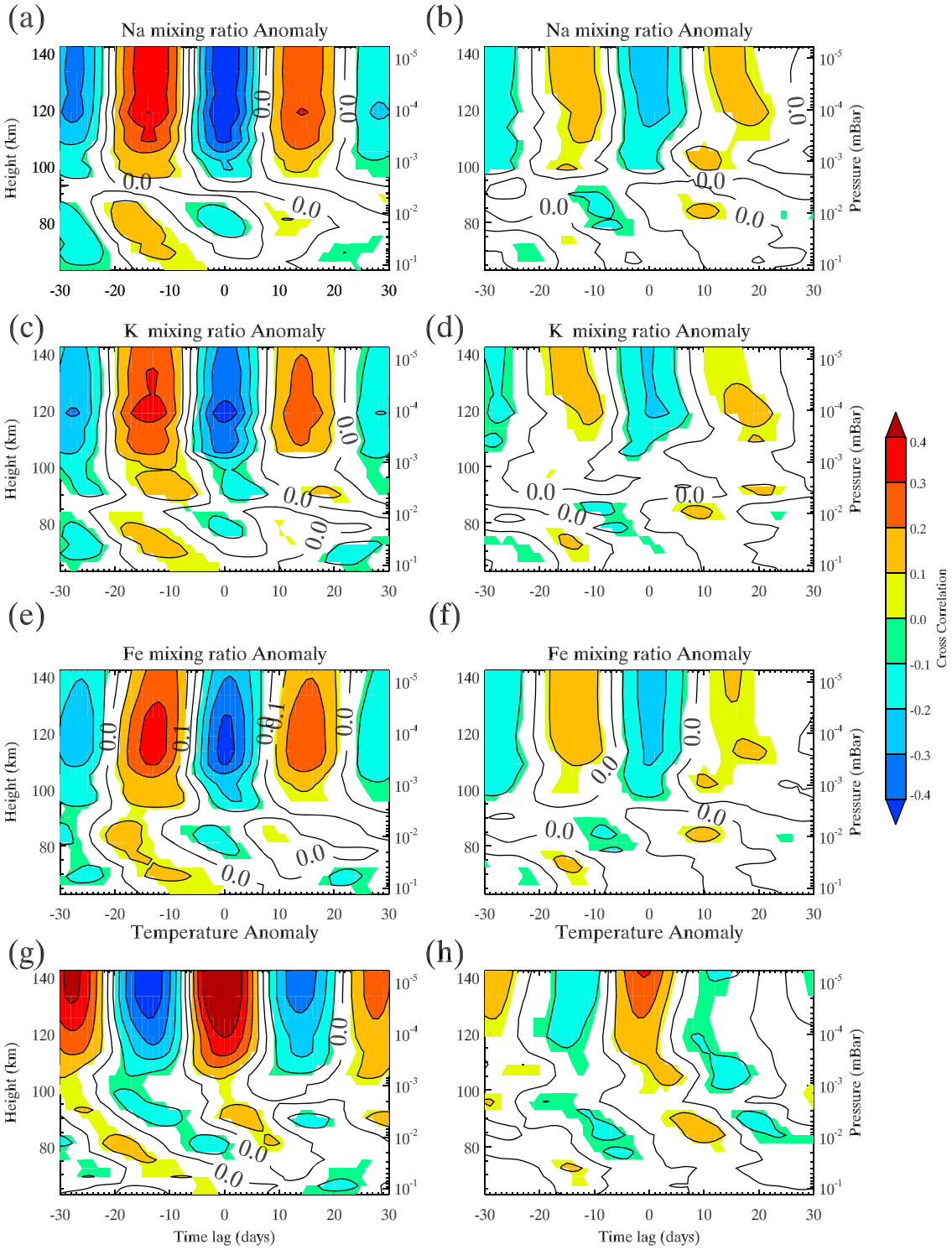

Figure 2. Cross-correlation functions between Whole Atmosphere Community Climate Model results and solar spectral irradiance at 121.5 nm as function of altitude and response time lag. Daytime for the solar maximum (left panel: a, c, e, and g) and minimum (right panel: b, d, f, and h). Colored areas: 99% confidence.

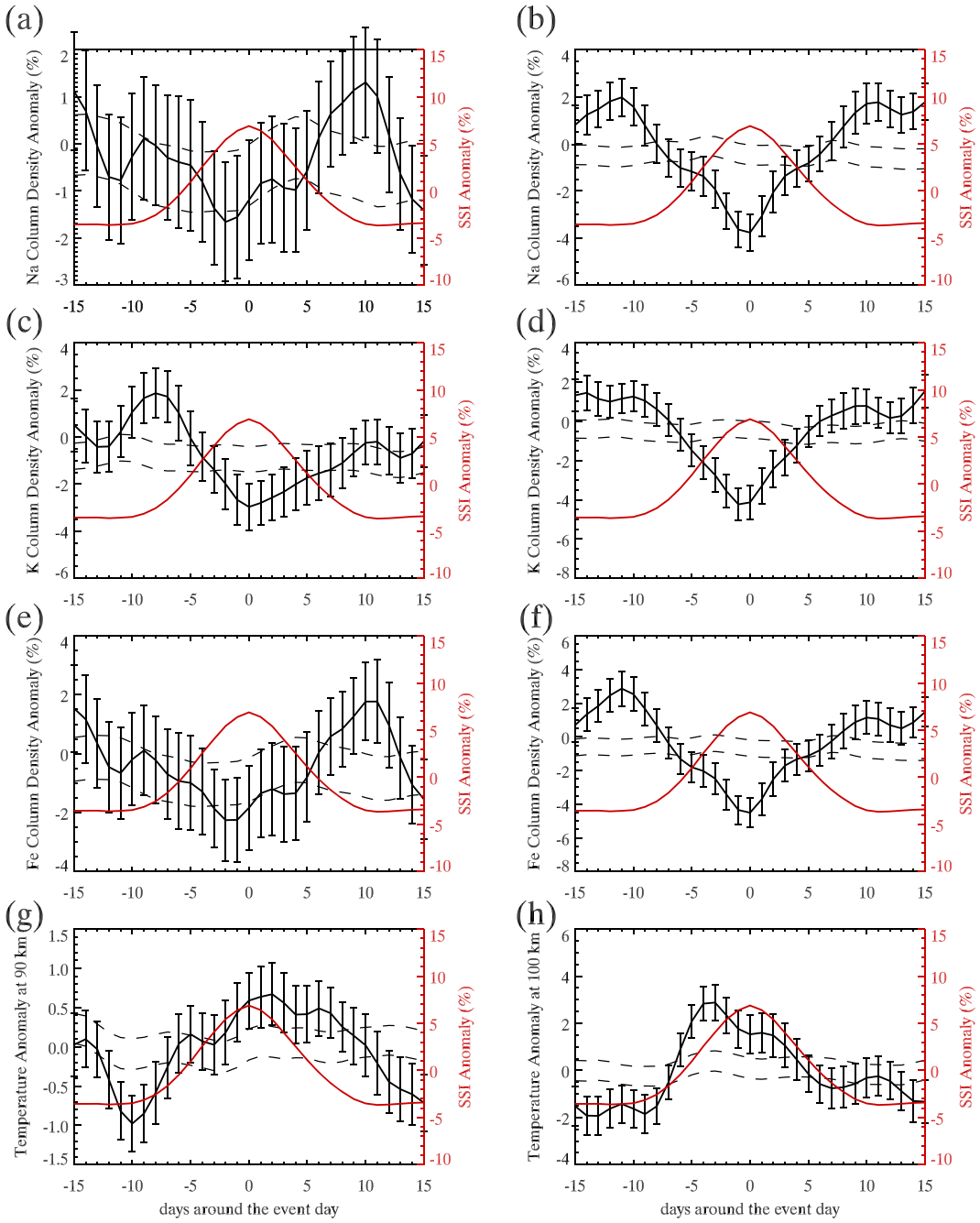

Figure 3. Superposed epoch analysis results of Whole Atmosphere Community Climate Model metal 27-day response with the standard error bars for Total Column Density (left panel) and partial Column Density above 100 km (right panel); dashed lines represents 99% confidence (see Text S1 for further details; Adams et al., 2003). SSI = solar spectral irradiance.

energies; Plane et al., 2015). This compensates for the neutral metal atoms lost by ionization, so that the overall response to solar radiation is not significant at the layer peaks but is positively correlated on the layer undersides (Figures 2a and 2e). In contrast, for K, the reaction $KHCO_3 + H$ has a very large activation energy and hence does not play a role at the low temperatures of the MLT (Plane et al., 2014). Thus, the K layer peak and solar radiation are anticorrelated. In comparison with solar maximum, the results for solar minimum (right panel of Figure 2) are significantly weaker. Therefore, in the rest of this study, we will focus on results from the period around solar maximum.

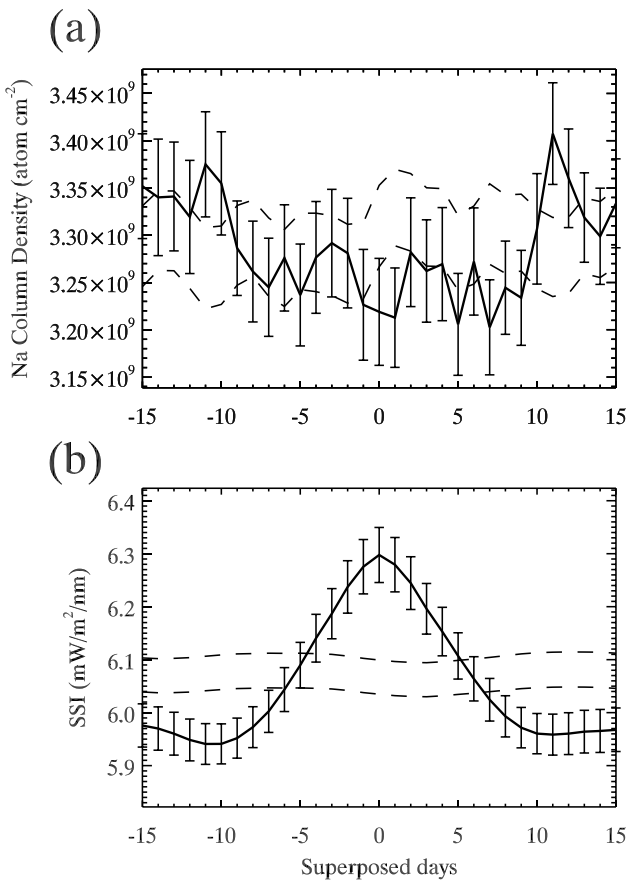

Figure 4. Superposed epoch analysis results of (a) Optical Spectrograph and InfraRed Imaging System Na 27-day response and (b) SSI at Lyman-alpha (121.5-nm wavelength), with the standard error bars during period of 2004–2013 over the tropics; dashed lines represents 95% confidence. SSI = solar spectral irradiance.

After demonstrating a clear response of the three metal layers to the 27-day solar cycle at each altitude, we now investigate the response in more detail. SEA (Chree, 1913) was applied to acquire a more quantifiable response to solar activity during solar maximum. This method is carried out in two stages, the first to find the local maxima of SSI to align the epochs and the second to average these epochs along with the data from day −15 to day +15 within each epoch. In this study, for the solar maximum of 1989–1994, we selected a total of 83 epochs for analysis. Figure 3 shows the superposed epoch anomalies of the calculated metal abundances and temperature anomalies. According to the vertical distribution of the metal layers, the total column density of each metal species (left panel of Figure 3) mostly reflects the response of the main layer, and the temperature anomaly at 90 km (Figure 3g) represents the actual temperature variability in the main metal layers. In general, Na, K, and Fe all exhibit a negative correlation with solar forcing. Considering the error bars, only the total column density of K is significant at the 99% level among the three metals, which is consistent with the conclusions drawn from Figure 2. The mean reduction of potassium at a time lag of 0 days is ~3%, corresponding to a ~7% increase in the SSI index.

As discussed in relation to Figure 2, there are significant anticorrelations between the metal atom densities and SSI above 100 km. Therefore, we also performed a SEA for the partial column density anomalies of the metal layers only above 100 km. The results are presented in the right panel of Figure 3, as well as the temperature anomaly at 100 km. All three metal anomalies are significantly negatively correlated with SSI anomaly, with a zero time lag, which is consistent with the previous conclusions (Figure 2). The epoch mean decrease of Na, K, and Fe atoms above 100 km is about 4% at 0-day time lag. Note that the temperature anomaly at 100 km reaches a maximum at day −3 and is not synchronized with the metal layers. This confirms that the ion chemistry in this region is largely independent of temperature (Plane et al., 2015).

The SEA method was then applied to OSIRIS Na raw data (also without a 3-day running mean smoothing) during the period of 2004–2013 over the tropics for a total of 65 epochs. As shown in Figure 4, a similar negative correlation with solar forcing is observed to that illustrated in Figure 3. Although the larger observational uncertainties (which arise because of the smaller size of the data set) mean that the correlation in Figure 4 is barely statistically significant, it nevertheless supports the modeled correlation and is the best that can be done with currently available observational data.

To make the correlation more robust, we applied the scatter diagram method to quantitatively determine the correlation between the 31 data points of the epoch averaged values of the SSI anomaly and the relative metal anomaly data sets, as well as the temperature anomaly. The Pearson correlation coefficient and linear regression were used to determine the statistical significance and sensitivity (see Figure S3). The sensitivity of the modeled partial column densities of Na, K, and Fe above 100 km with respect to the SSI index data are −0.46% (±0.04%)/(1% SSI index), −0.46% (±0.04%)/(1% SSI index), and −0.52% (±0.05%)/(1% SSI index), respectively. The sensitivity of the Na, K, and Fe responses determined by the slope of the fitted line at each altitude as a function of altitude for the solar maximum period is illustrated in Figure S4. In the peak layer (~90 km), only potassium exhibits a significant anticorrelation with a sensitivity value of approximately −0.3%/(1% SSI index). Above 100 km, Na, K, and Fe show similar sensitivity values and trends. The maximum sensitivity value reaches approximately −1% at these higher altitudes.

4. Conclusions

The response of the Na, K, and Fe layers to the 27-day solar rotational cycle has been investigated by using the WACCM model with added metal chemistry. This is the first time that the solar-driven 27-day variation

of the metal layers in the MLT region has been identified. The following features of the MLT response of metal layers are noteworthy: (1) The metal response is significantly stronger during solar maximum than solar minimum. (2) Above 100 km, the significant anticorrelation of the metal layers with SSI is explained by the role of ion-molecule chemistry (Plane et al., 2015). (3) At the metal layer peaks, only K shows a small anticorrelation within error, which is consistent with the response of the K layer to the 11-year solar cycle (Dawkins et al., 2016). The only available observational data of the Na layer made by the spaceborne OSIRIS instrument also shows a weak anticorrelation to the 27-day solar rotational cycle during 2004–2013, which is consistent with the WACCM analysis.

To our knowledge, there have been no previous studies of the response to the 27-day solar cycle of the metals layers, either from observations or simulations in the MLT. The sensitivities of the metal layer responses are comparable to the O_3 (Gruzdev et al., 2009, and references therein) and OH and H_2O (Shapiro et al., 2012) responses in the MLT. Moreover, in the thermosphere above 100 km, where there is growing interest in the metal layers and their response to solar activity (Chu et al., 2011; Gao et al., 2015; Xue et al., 2013; Wang et al., 2012), the model sensitivity is greater than −0.5%/(1% SSI). It is desirable that the response of the metal layers to solar activity in the thermosphere should be further investigated with continuous high-resolution lidar measurements and chemical-dynamical models coupled containing ionospheric physics.

Acknowledgments
This work was supported by the National Natural Science Foundation of China (41704148 and 41774158) and the Open Research Project of Large Research Infrastructures of CAS—"Study on the interaction between low/mid-latitude atmosphere and ionosphere based on the Chinese Meridian Project." W. F. and J. M. C. P. were funded by the European Research Council CODITA project (291332), and the WACCM model output and OSIRIS data have been archived at the Leeds University PetaByte Environmental Tape Archive and Library (https://www.environment.leeds.ac.uk/wiki/view/IT/PetalArchive). The National Center for Atmospheric Research is sponsored by the National Science Foundation.

References

Adams, J. B., Mann, M. E., & Ammann, C. M. (2003). Proxy evidence for an El Niño-like response to volcanic forcing. *Nature*, *426*, 274–278.

Chree, C. (1913). Some phenomena of sunspots and of terrestrial magnetism at Kew observatory, Philosophical Transactions of the Royal Society of London. Series A. *Containing Papers of a Mathematical or Physical Character*, *212*, 75–116.

Chu, X., Yu, Z., Gardner, C. S., Chen, C., & Fong, W. (2011). Lidar observations of neutral Fe layers and fast gravity waves in the thermosphere (110-155 km) at McMurdo (77.8°S, 166.7° E), Antarctica. *Geophysical Research Letters*, *38*, L23807. https://doi.org/10.1029/2011GL050016

Dawkins, E. C. M., Plane, J. M. C., Chipperfield, M. P., Feng, W., Gumbel, J., Hedin, J., et al. (2014). First global observations of the mesospheric potassium layer. *Geophysical Research Letters*, *41*, 5653–5661. https://doi.org/10.1002/2014GL060801

Dawkins, E. C. M., Plane, J. M. C., Chipperfield, M. P., Feng, W., Marsh, D. R., Höffner, J., & Janches, D. (2016). Solar cycle response and long-term trends in the mesospheric metal layers. *Journal of Geophysical Research: Space Physics*, *121*, 7153–7165. https://doi.org/10.1002/2016JA022522

Fan, Z. Y., Plane, J. M. C., Gumbel, J., Stegman, J., & Llewellyn, E. J. (2007). Satellite measurements of the global mesospheric sodium layer. *Atmospheric Chemistry and Physics*, *7*(15), 4107–4115. https://doi.org/10.5194/acp-7-4107-2007

Feng, W., Marsh, D. R., Chipperfield, M. P., Janches, D., Höeffner, J., Yi, F., & Plane, J. M. C. (2013). A global atmospheric model of meteoric iron. *Journal of Geophysical Research: Atmospheres*, *118*, 9456–9474. https://doi.org/10.1002/jgrd.50708

Gao, Q., Chu, X., Xue, X., Dou, X., Chen, T., & Chen, J. (2015). Lidar observations of thermospheric Na layers up to 170 km with a descending tidal phase at Lijiang (26.7°N, 100.0°E), China. *Journal of Geophysical Research: Space Physics*, *120*, 9213–9220. https://doi.org/10.1002/2015ja021808

Gruzdev, A. N., Schmidt, H., & Brasseur, G. P. (2009). The effect of the solar rotational irradiance variation on the middle and upper atmosphere calculated by a three-dimensional chemistry-climate model. *Atmospheric Chemistry and Physics*, *9*(2), 595–614. https://doi.org/10.5194/acp-9-595-2009

Gumbel, J., Fan, Z. Y., Waldemarsson, T., Stegman, J., Witt, G., Llewellyn, E. J., et al. (2007). Retrieval of global mesospheric sodium densities from the Odin satellite. *Geophysical Research Letters*, *34*, L04813. https://doi.org/10.1029/2006GL028687

Hurrell, J. W., Holland, M. M., Gent, P. R., Ghan, S., Kay, J. E., Kushner, P. J., et al. (2013). The Community Earth System Model: A framework for collaborative research. *Bulletin of the American Meteorological Society*, *94*(9), 1339–1360. https://doi.org/10.1175/BAMS-D-12-00121.1

Keating, G. M., Pitts, M. C., Brasseur, G., & De Rudder, A. (1987). Response of middle atmosphere to short-term solar ultraviolet variations: 1. Observations. *Journal of Geophysical Research*, *92*(D1), 889–902. https://doi.org/10.1029/JD092iD01p00889

Lean, J., Rottman, G., Harder, J., & Kopp, G. (2005). SORCE contributions to new understanding of global change and solar variability. *Solar Physics*, *230*(1-2), 27–53. https://doi.org/10.1007/s11207-005-1527-2

Lednyts'kyy, O., von Savigny, C., & Weber, M. (2017). Sensitivity of equatorial atomic oxygen in the MLT region to the 11-year and 27-day solar cycles. *Journal of Atmospheric and Solar-Terrestrial Physics*, *162*, 136–150. https://doi.org/10.1016/j.jastp.2016.11.003

Marsh, D. R., Janches, D., Feng, W. H., & Plane, J. M. C. (2013). A global model of meteoric sodium. *Journal of Geophysical Research: Atmospheres*, *118*, 11,442–11,452. https://doi.org/10.1002/jgrd.50870

Marsh, D. R., Mills, M. J., Kinnison, D. E., Lamarque, J.-F., Calvo, N., & Polvani, L. M. (2013). Climate change from 1850 to 2005 simulated in CESM1 (WACCM). *Journal of Climate*, *26*, 7372–7391. https://doi.org/10.1175/JCLI-D-12-00558.1

Plane, J. M. C., Feng, W., & Dawkins, E. C. M. (2015). The mesosphere and metals: Chemistry and changes. *Chemical Reviews*, *115*(10), 4497–4541. https://doi.org/10.1021/cr500501m

Plane, J. M. C., Feng, W., Dawkins, E., Chipperffeld, M. P., Höffner, J., Janches, D., & Marsh, D. R. (2014). Resolving the strange behavior of extraterrestrial potassium in the upper atmosphere. *Geophysical Research Letters*, *41*, 4753–4760. https://doi.org/10.1002/2014gl060334

Robert, C. E., von Savigny, C., Rahpoe, N., Bovensmann, H., Burrows, J. P., De- Land M. T., & Schwartz, M. J. (2010). First evidence of a 27 day solar signature in noctilucent cloud occurrence frequency. *Journal of Geophysical Research*, *115*, D00I12. https://doi.org/10.1029/2009JD012359

Shapiro, A. V., Rozanov, E., Shapiro, A. I., Wang, S., Egorova, T., Schmutz, W., & Peter, T. (2012). Signature of the 27-day solar rotation cycle in mesospheric OH and H_2O observed by the Aura Microwave Limb Sounder. *Atmospheric Chemistry and Physics*, *12*(7), 3181–3188. https://doi.org/10.5194/acp-12-3181-2012

Singh, A. K., & Tonk, A. (2014). Solar activity during first six years of solar cycle 24 and 23: A comparative study. *Astrophysics and Space Science*, *353*, 367–371. https://doi.org/10.1007/s10509-014-2067-8

Thurairajah, B., Thomas, G. E., von Savigny, C., Snow, M., Hervig, M. E., Bailey, S. M., & Randall, C. E. (2017). Solar-induced 27-day variations of polar mesospheric clouds from the AIM SOFIE and CIPS experiments. *Journal of Atmospheric and Solar-Terrestrial Physics*, *162*, 122–135. https://doi.org/10.1016/j.jastp.2016.09.008

Torrence, C., & Compo, G. P. (1998). A practical guide to wavelet analysis. *Bulletin of the American Meteorological Society*, *79*(1), 61–78. https://doi.org/10.1175/15200477(1998)079h0061:APGTWAi2.0.CO;2

von Savigny, C., Eichmann, K., Robert, C. E., Burrows, J. P., & Weber, M. (2012). Sensitivity of equatorial mesopause temperatures to the 27-day solar cycle. *Geophysical Research Letters*, *39*, L21804. https://doi.org/10.1029/2012GL053563

von Savigny, C., Peters, D. H. W., & Entzian, G. (2019). Solar 27-day signatures in standard phase height measurements above central Europe. *Atmospheric Chemistry and Physics*, *19*(3), 2079–2093. https://doi.org/10.5194/acp-19-2079-2019

Wang, J., Yang, Y., Cheng, X., Yang, G., Song, S., & Gong, S. (2012). Double sodium layers observation over Beijing, China. *Geophysical Research Letters*, *39*, L15801. https://doi.org/10.1029/2012GL052134

Xue, X. H., Dou, X. K., Lei, J., Chen, J. S., Ding, Z. H., Li, T., et al. (2013). Lower thermospheric-enhanced sodium layers observed at low latitude and possible formation: Case studies. *Journal of Geophysical Research: Space Physics*, *118*, 2409–2418. https://doi.org/10.1002/jgra.50200

Yigit, E., Knízová, P. K., Georgieva, K., & Ward, W (2016). A review of vertical coupling in the atmosphere–ionosphere system: Effects of waves, sudden stratospheric warmings, space weather, and of solar activity. *Journal of Atmospheric and Solar-Terrestrial Physics*, *141*, 1–12. https://doi.org/10.1016/j.jastp.2016.02.011